Microstructures of ramp-edge $YBa_2Cu_3O_x/PrBa_2Cu_3O_x/YBa_2Cu_3O_x$ Josephson junctions on different substrates

J.G. Wen [a,*], N. Koshizuka [a], C. Traeholt [b], H.W. Zandbergen [b], E.M.C.M. Reuvekamp [c,1], H. Rogalla [c]

[a] *Superconductivity Research Laboratory, ISTEC, 1-10-13 Shinonome, Koto-ku, Tokyo 135, Japan*
[b] *National Center for HREM, Delft University of Technology, Rotterdamseweg 137, 2628 AL Delft, The Netherlands*
[c] *Department of Applied Physics, University of Twente, PO Box 217, 7500 AE Enschede, The Netherlands*

Abstract

Ramp-edge $YBa_2Cu_3O_x/PrBa_2Cu_3O_x/YBa_2Cu_3O_x$ Josephson junctions with $PrBa_2Cu_3O_x$ (PrBCO) or $SrTiO_3$ as a separating layer on different kinds of substrate have been studied by high-resolution electron microscopy. The bottom $YBa_2Cu_3O_x$ (YBCO) layer and the separating layer (PrBCO or $SrTiO_3$) were epitaxially c oriented, irrespective of the substrate (yttria stabilized zirconia (YSZ), $SrTiO_3$ or $NdGaO_3$, all in (001) orientation). The use of ion milling in the manufacturing of Josephson junctions was found to yield smooth slopes with an angle of about 20°. The Josephson junction was facing away from the beam direction was found to have a dimple in the substrate near the base of the junction. The barrier layers were observed to have a homogeneous thickness. These layers as well as the top YBCO layers were oriented with their c-axes perpendicular to (001) plane of the substrate for perovskite substrates and perpendicular to the surface for YSZ substrates. In the case of a YSZ substrate, the dimple in the substrate as well as the slope of the substrate close to the base of the junction were found to lead to small-angle grain boundaries in the YBCO film as well as randomly oriented YBCO grains, which results in a poor ramp-edge junction. In the case of $SrTiO_3$ or $NdGaO_3$ substrate, all components of the device were fully epitaxial, thus resulting in good ramp-edge junctions.

1. Introduction

There have been numerous attempts to develop high-T_c Josephson junctions [1]. The most common

are grain-boundary junctions artificially created in epitaxial films such as bicrystal substrate junctions [2], bi-epitaxial junctions [3], and step-edge junctions [4]. Another type of junction consists of a trilayer structure in which an insulting or normal-conducting barrier layer is sandwiched between two superconducting layers. A YBCO/PrBCO/YBCO sandwich is an example of such type of junction. Because most high-quality YBCO thin films are c-axis oriented,

---

* Corresponding author.
[1] Present address: Philips Analytical X-ray Tubes, Achtsweg Noord 5, 5651 GG Eindhoven, The Netherlands.
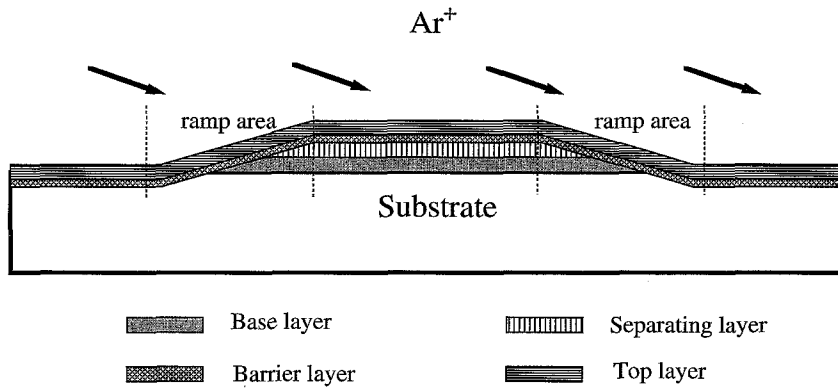
Fig. 1. The schematic geometry of a pair of ramp-edge junctions in a multi-junction sample. The Ar^+ ions are incident from the left during the JJ ion milling resulting in junctions facing towards and away from the ion milling.

the ramp-edge type multilayer junction utilizes the ramp edge of the epitaxial multilayer to form the weak link, as shown in Fig. 1. This type of junction geometry is chosen because the superconducting co-herence length perpendicular to the c-axis is much longer than that parallel to the c-axis, such that the optimal direction for tunneling is in the ab plane. In this study the two electrodes are superconducting

Fig. 2. A TEM image of a ramp-edge junction DyBCO/PrBCO/PrBCO/DyBCO on a $SrTiO_3$ substrate facing towards the JJ ion gun. The interfaces between the layers are indicated by solid white lines. The horizontal lines correspond to (001) fringes with a spacing 1.17 nm. The barrier layer is indicated by two black arrow heads. All components of the device are c oriented and epitaxial to the [001] direction of the substrate. A substrate ramp can be observed.

YBCO or DyBCO layers. The separating layer, which separates the two YBCO layers along the substrate normal, is a PrBCO layer or a $SrTiO_3$ layer. It should be thick enough to avoid Josephson coupling between two superconducting layers. The thickness (homogeneous, ultrathin) and quality (homogeneous, no pinholes, no local reaction with YBCO, no dislocations due to lattice mismatch between neighboring superconducting layers) of the barrier layer in this type of junction needs to be well controlled since they determine the performance of the junction. If the thickness and quality of the barrier layer can be well controlled, ramp-edge junctions may become of importance for future superconductive electronic developments. In this paper we use a short-hand notation for the junction according to the growth sequence: "base layer/separating layer/barrier layer/top layer".

A study of the microstructure of the ramp-edge junction YBCO/PrBCO/PrBCO/YBCO has only been reported by Lebedev et al. [5]. They reported that the bottom and separating layers are c oriented films. The barrier layer and the top layer are full of defects, which was explained by the need to break the vacuum needed for the deposition and removal of the photoresist before depositing the barrier layer and the top layer.

A high-resolution electron microscopy (HREM) study of step junctions has been reported by Jia et al. [6]. They have presented a systematic HREM study of the microstructure of epitaxial YBCO films on steep steps on $LaAlO_3$ substrate. Jia et al. [7] also reported a HREM study of the microstructure of YBCO on a step-edge $SrTiO_3$ substrate. Their results indicate that one needs a step with a high-angle slope ($> 45°$) to produce a step-edge junction. In this case one obtains two [100] 90° rotation twin boundaries. On a step with a low-angle slope, the film grows
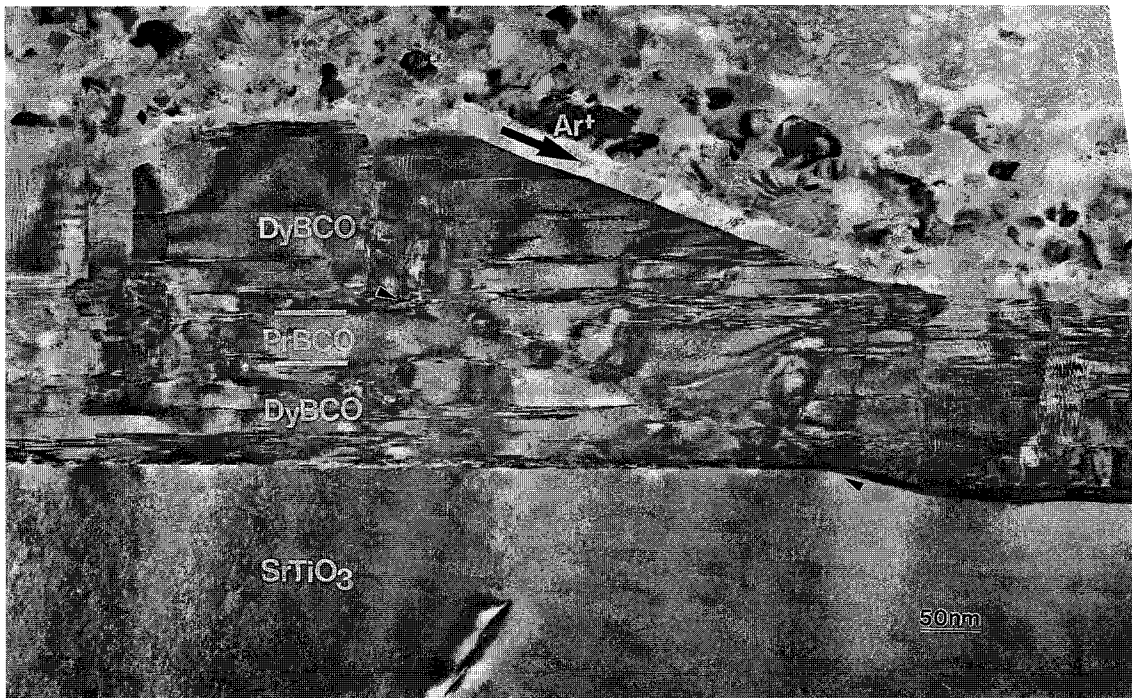

Fig. 3. A TEM image of a ramp-edge junction DyBCO/PrBCO/PrBCO/DyBCO on a $SrTiO_3$ substrate but now facing away from the JJ ion gun. The barrier layer can clearly be seen indicated by two black arrow heads. A few microcracks can be observed in the four-layer part which does not influence the property of the junction. A substrate ramp and a dimple can be observed in the substrate.

without any change in c-axis orientation across the step and without grain boundaries. This result is in agreement with our observations of large steps on SrTiO$_3$ [8].

In the present paper we present a systematic cross-sectional HREM study of ramp-edge junctions on various substrates. Results on the physical properties of these junctions are presented elsewhere [9].

2. Experimental

The ramp-edge junctions were fabricated according to the geometry shown schematically in Fig. 1. The fabrication sequence begins with the deposition of the YBCO (or DyBCO) base electrode and the separating layer PrBCO (or SrTiO$_3$). The separating layer PrBCO (or SrTiO$_3$) is made thick enough to avoid Josephson coupling and short circuiting be-

tween two YBCO layers along the c-axis direction. Since SrTiO$_3$ is insulating and PrBCO is semiconducting, the required thickness of a SrTiO$_3$ separation is much less than that for PrBCO layer. After the deposition of the base YBCO and the separating layer, the sample is removed from the deposition chamber and a part of the multilayer is covered by a photo-resist stencil. The unprotected area is etched by an argon ion beam with an incident angle (less than 20°) in order to fabricate a ramp. This ion-milling process will be called "JJ (Josephson junction) ion milling" in the rest of this paper. After removing the photo-resist stencil, the surface is cleaned with an Ar$^+$ ion beam before depositing the barrier layer. A thin PrBCO barrier layer and YBCO (or DyBCO) top layer are deposited subsequently. More details on the manufacturing conditions of these films are reported by Gao et al. [10,11].

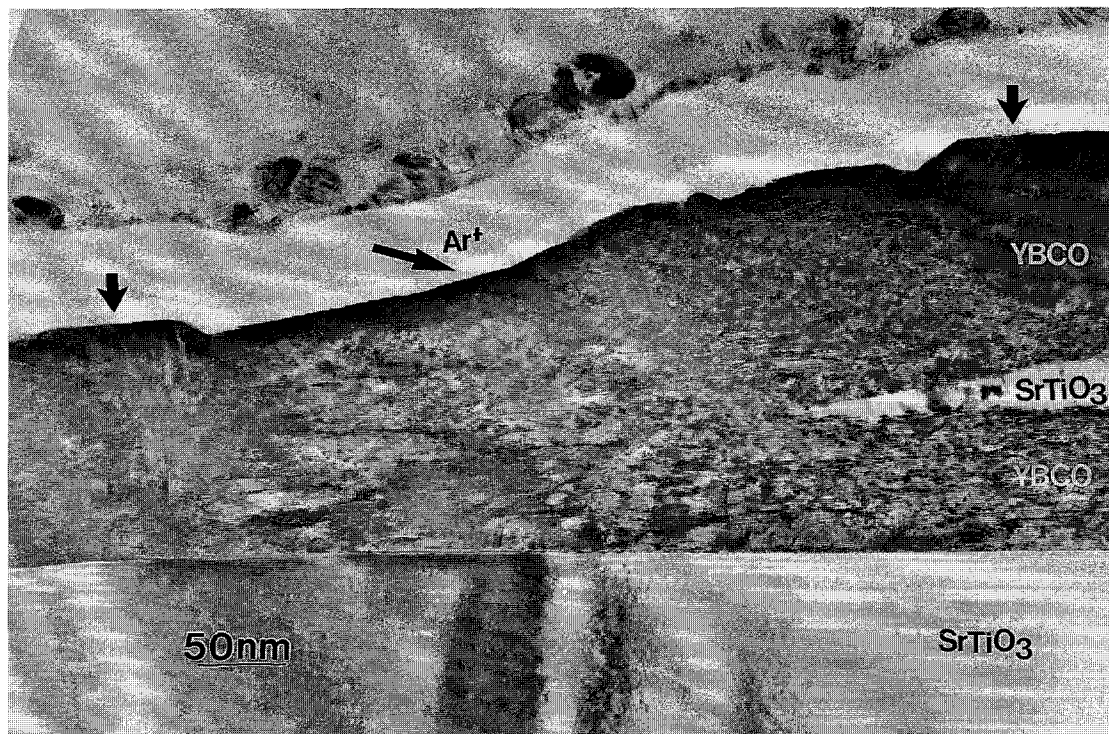Various kinds of samples were investigated:

Fig. 4. A ramp-edge junction YBCO/SrTiO$_3$/PrBCO/YBCO on a SrTiO$_3$ substrate facing towards the JJ ion gun. Some a oriented grains (indicated by black arrows) can be seen at the bottom and the top of the ramp.
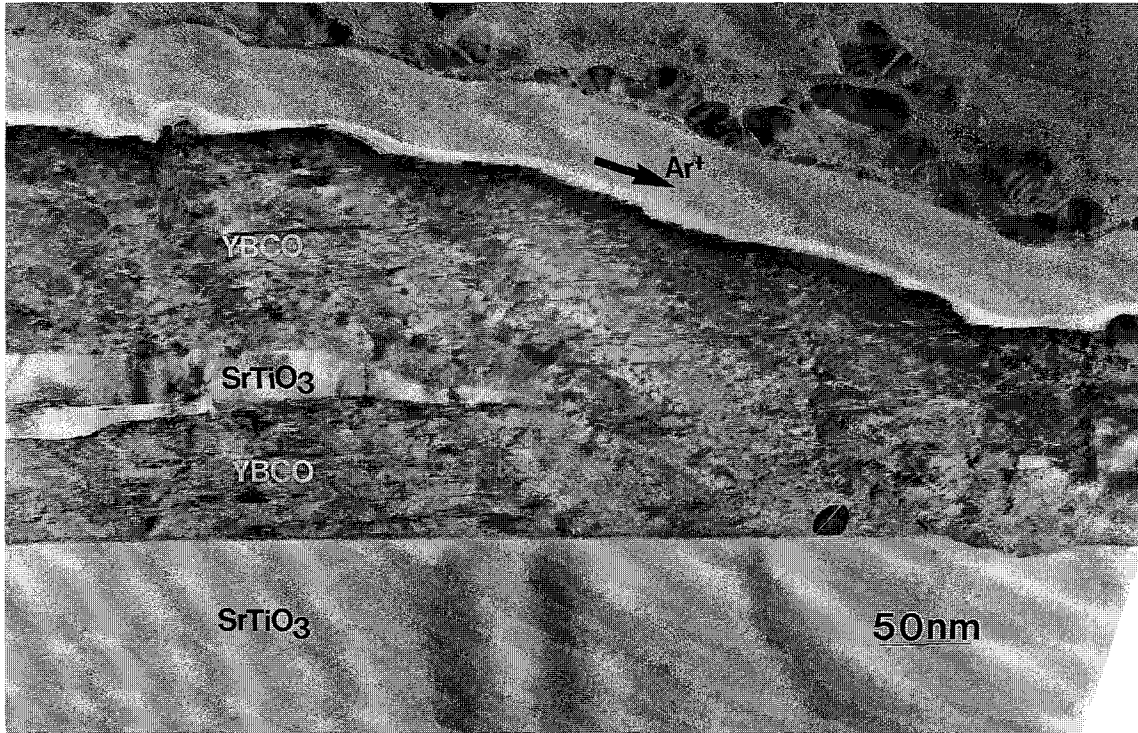
Fig. 5. A ramp-edge junction which is facing away from the JJ ion gun from the same sample as shown in Fig. 4. The barrier layer with a homogeneous thickness can be seen clearly (also see Fig. 6). There is a dimple on the substrate at the bottom of the ramp. PrBCO film is epitaxially grown on this dimple. The dark particle is an unknown second phase.
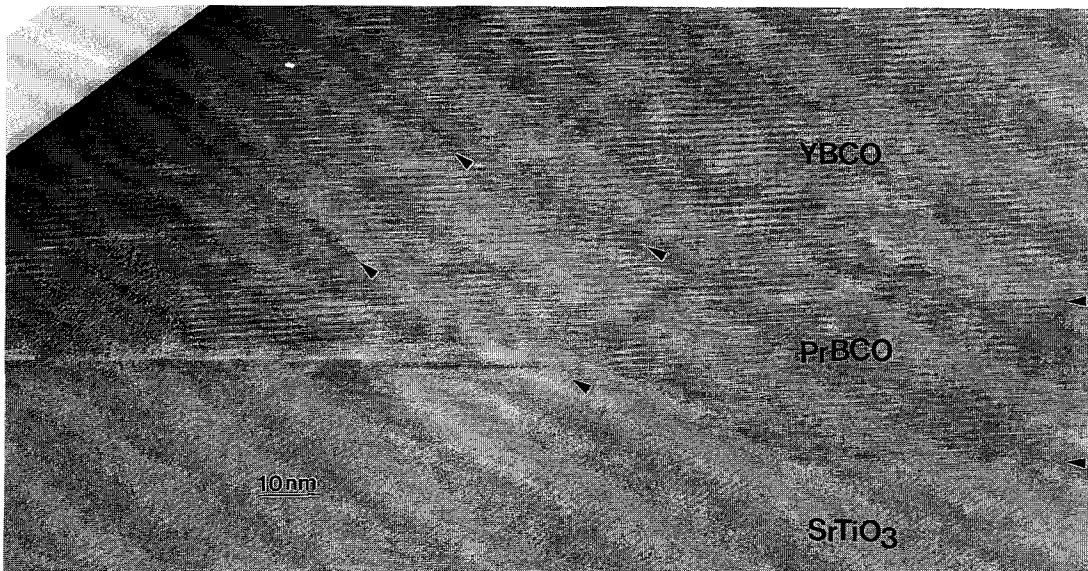

Fig. 6. An enlargement of Fig. 5 showing the epitaxy of the PrBCO barrier layer on the dimple in the $SrTiO_3$ substrate. The barrier layer is indicated by black arrow heads. The angle between the interface and (001) plane of $SrTiO_3$ is about 20°. A second phase is visible in the left upper part of the figure.

(1) a multi-junction DyBCO/PrBCO/PrBCO/Dy-BCO on a $SrTiO_3$ substrate,

(2) a multi-junction DyBCO/PrBCO/PrBCO/Dy-BCO on a $NdGaO_3$ substrate,

(3) a multi-junction YBCO/$SrTiO_3$/PrBCO/YBCO on a $SrTiO_3$ substrate,

(4) a single YBCO/PrBCO/PrBCO/YBCO junction on a YSZ substrate (40 μm wide).

The first three specimens were specially made for HREM investigations such that they contains many junctions (multi-junction). The last specimen contained only a single junction.

A cross-section specimen for transmission electron microscopy was first mechanically ground directly down to a thickness less than 10 μm. For further thinning by ion milling the specimen was mounted on a single hole copper grid (with diameter 0.8 mm). This ion milling will be called "CS (cross-section) ion milling" in the rest of the paper. During CS ion milling (Gatan duo mill 600), the specimen was not rotated and was oriented such that the thin-film side was facing away from the ion gun. By using this method, the substrate $SrTiO_3$ or YSZ was used as an ion-beam block to minimize preferential milling of the YBCO thin film. The CS ion-mill-ing conditions were acceleration voltage 4.5 kV, gun current 0.5 mA, ion milling angle 15° and no liquid-nitrogen cooling. When color fringes (thin-film reflection) appeared on the edge of the specimen an ion-polishing procedure was applied to thin the specimen to electron transparency with conditions: acceleration voltage 3 kV, gun current 0.3 mA, ion milling angle 8°. This specimen-preparation technique provides large thin areas which enables one to investigate the thin-film quality by HREM over an area of more than 200 μm. Details on the sample preparation have already been published elsewhere [12].

Electron microscopy was performed with a Philips CM30ST electron microscope operating at 300 kV and equipped with a field emission gun and a side-entry ±25° tilt specimen holder. The HREM images were recorded at a focus about −40 nm at which all cations are imaged as dark dots, provided the specimen is thin enough, and/or at about −80 nm where the cations are imaged as white dots. Having a similar structure, the contrast difference between YBCO (DyBCO) and PrBCO is small. In this case the contrast was enhanced by imaging in a direction which is not parallel to a low-index zone. In order to distinguish the thin barrier layer with YBCO (Dy-
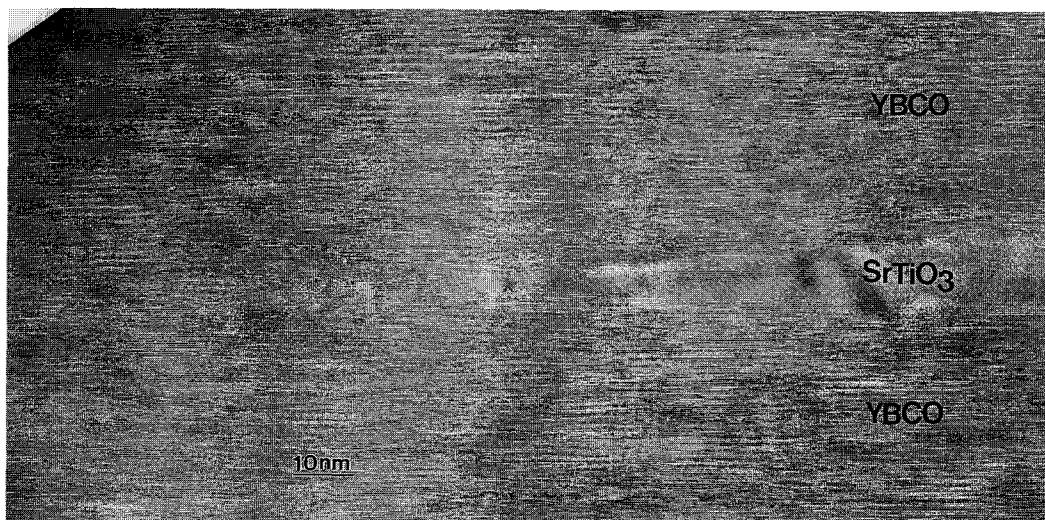

Fig. 7. An enlargement of the tip of the separating layer at the Josephson junction of Fig. 4. The PrBCO barrier layer and the top YBCO layer grow epitaxially on the inclined $SrTiO_3$ surface. No a oriented grains and other defects are visible.

BCO), the film was tilted about 5° away from the [001] zone axis, such that the c plane of the film was not parallel with the beam direction.

3. Results

Figs. 2 and 3 show cross-section TEM images (same sample) of two ramp-edge junctions in a multi-layer DyBCO/PrBCO/PrBCO/DyBCO on a (001) SrTiO$_3$ substrate. During JJ ion milling these junctions faced towards and away from the ion gun, respectively, equivalent to the left and right ramp in Fig. 1. The thickness of the bottom DyBCO and the top DyBCO layers are about 80 nm and 150 nm, respectively. The separating PrBCO layer is about 60 nm. In Fig. 2 the interface between the barrier and the bottom DyBCO layer is clearly visible while the

other interface (top) of the barrier is difficult to distinguish, i.e. the thickness of the barrier layer cannot be determined precisely. In Fig. 3 one can clearly see the barrier which has a thickness of about 8 nm. All components of the film are c oriented and are epitaxial to the [001] direction of the substrate. The slope of the junction is about 20° in agreement with the ion-milling angle which was used in the JJ ion milling. The continuous (001) lattice fringes which cross the junction area without bending indicate that the barrier layer has the same orientation as the neighboring DyBCO layers and that no discontinuities occur in the lattice. The horizontal lines with bright contrast in the film correspond to the stacking faults such as double CuO layers. In the top DyBCO layer in Figs. 2 and 3 some weak vertical lines are visible which correspond to defects such as antiphase boundaries and microcracks due to the improper
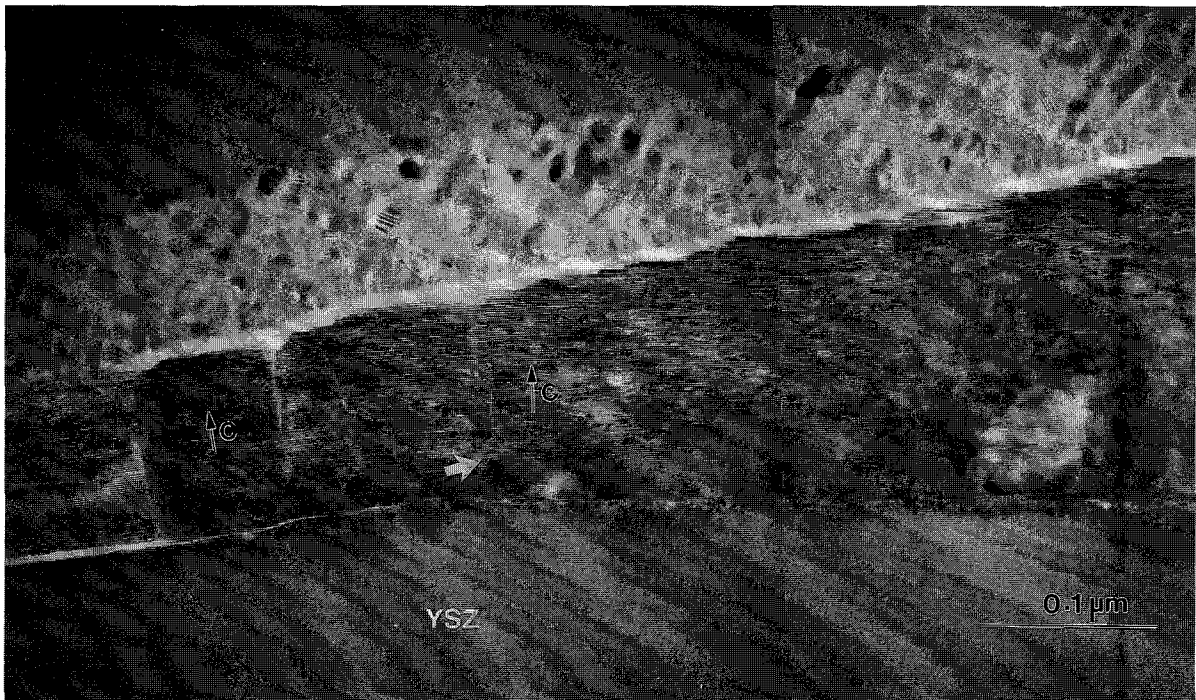

Fig. 8. A TEM image of a YBCO/PrBCO/PrBCO/YBCO ramp-edge junction on YSZ substrate. As the c-axis of the film is perpendicular to the inclined surface, there is an 8° misalignment between the left and the right part of the film. Here the difference is accommodated by the presence of one grain boundary and a few microcracks. An a-axis oriented YBCO grain is formed in the junction area, which results in an a-axis grain in the top YBCO film.

growth condition for the top layer. In Fig. 3 a clear example of a microcrack can be seen. The formation of these cracks is subject to further research.

In the top part of the image in Figs. 2 and 3 some material can be observed which was deposited on the surface of the film during the CS ion milling. This deposition is not removed during the further CS ion milling because it is shadowed by the specimen. The interface between this material and the DyBCO top layer is sharp and can be used to locate the surface of the device, since the method of CS ion milling allows the surface to keep its original shape without being damaged. The top DyBCO layer is quite smooth in the four-layer part as well as in the two-layer part. The surface of the top DyBCO layer in the ramp area follows the shape of the ramp created by the JJ ion milling. In this sample the interfaces at the ramp, (i.e. the interfaces between the barrier and the bottom, the top and the separating layers), are quite smooth.

In order to be certain that the bottom DyBCO layer is completely removed during the JJ ion milling usually a little more JJ ion milling is done, thus removing some of the substrate material. This leads to an extension of the ramp into the substrate (substrate ramp) as can be seen in Fig. 2. The thickness of the removed substrate is 15 nm except for the region close to the junction where the substrate is inclined. From Fig. 2 one can measure that the angle of the slope in the substrate ramp is about 10°, whereas the slope in the film ramp is about 20°. In Fig. 3 the amount of the removed substrate is 25 nm which is more than that in Fig. 2. The angle of the slopes of the ramps in the film and the substrate are about 23° and 15°, respectively. In Fig. 3 a very thin shallow dimple can be observed in the substrate at the base of the ramp.

Figs. 4 and 5 show two ramp-edge junctions of the systems $YBCO/SrTiO_3/PrBCO/YBCO$ on $SrTiO_3$ (same sample) facing towards and facing
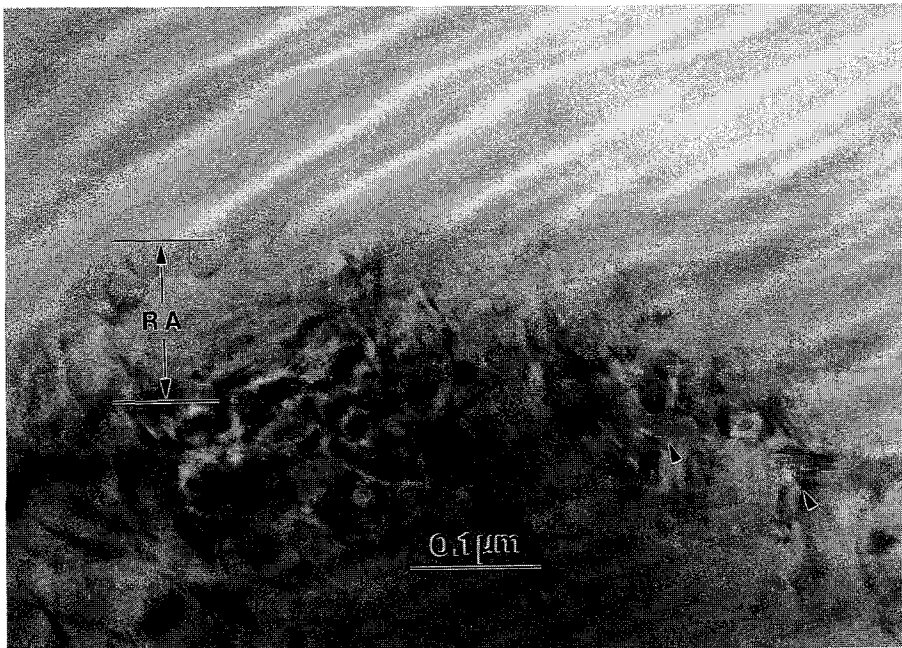

Fig. 9. A low-magnification plan-view TEM image of the ramp-edge junction from the same sample as shown in Figs. 2 and 3. Within the ramp area (1 μm along the horizontal direction and 0.1 μm along the width of the ramp), the film shows no defect except some *a* orientated grains (indicated by arrow heads) in the four-layer film.

away from the ion gun, respectively. The thicknesses of the bottom layer, separating layer, and the top layer are 80 nm, 30 nm, and 130 nm, respectively. The barrier layer is PrBCO with a thickness of about 20 nm. The PrBCO/YBCO interfaces appear as bands of dark contrast (see Fig. 6). The PrBCO barrier layer and the top YBCO layer on both junctions show epitaxial growth in the ramp area. Also on the inclined ramp surface of the separating $SrTiO_3$ layer the PrBCO barrier layer grows epitaxially. The interfaces in the ramp area are not smooth in Fig. 5. This can be seen from the surface of the top YBCO film in the ramp area. Some *a* oriented grains can be observed in the top YBCO layer in the two layer area as well as the four layer area (see Figs. 4 and 5).

The bottom layer was found to contain second phases (see Fig. 5).

Several differences between Figs. 4 and 5 can be observed. In the first place a dimple on the substrate can be observed in Fig. 5. The depth of the dimple is 6 nm whereas the slope angles are 20° on the ramp side and 18° on the other side. The slope of the substrate ramp in Fig. 5 is about 20°. Secondly, 5 nm of substrate at the ramp facing the ion gun is removed by the JJ ion milling whereas 13 nm is removed on the other side. A third difference is that the barrier layer only can be seen clearly in Fig. 5.

Fig. 6 is an enlargement of Fig. 5 showing the epitaxy of the barrier PrBCO layer on the dimple in the $SrTiO_3$ substrate. The angle between the inter-
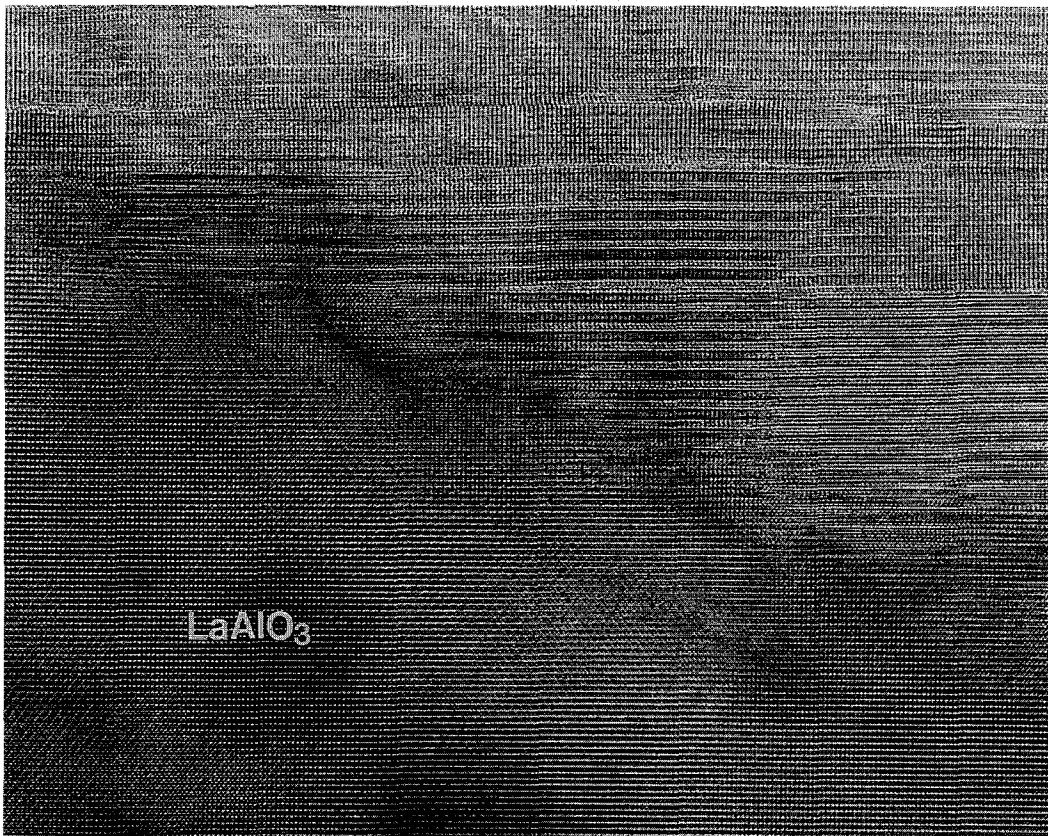

Fig. 10. An YBCO thin film can epitaxially grow on a step with step angle less than 40° of perovskite-like substrate with its (001) plane parallel to that of the substrate.

face and the (001) plane of SrTiO₃ is about 20° (angle due to JJ ion milling). Along the whole interface (around 2 nm for the area at the dimple and 1 nm for the rest) the image shows a contrast which does not resemble the structure of SrTiO₃ nor that of YBCO. About 2 nm from the interface the substrate image in the film corresponds to that of YBCO structure and is predominately perfect.

Fig. 7 shows an enlargement of the tip of the separating layer at the Josephson junction of Fig. 4. It is easily seen that the PrBCO barrier layer and the YBCO top layer grow epitaxially on the inclined SrTiO₃ surface. The slope angle is about 10° although the JJ ion milling angle was 20°. This may be related to the relative low ion-milling rate of SrTiO₃.

Fig. 8 shows a low-magnification image of a

Fig. 11. An YBCO thin film grows on a step with step angle around 45° with a mix of *a* and *c* oriented grains.

cross-section of a YBCO/PrBCO/PrBCO/YBCO ramp-edge junction on a YSZ substrate. This single junction (width 40 μm) was pinpointed on a 10 mm × 10 mm chip. It shows that it is possible to locate a single junction and thin it down to electron transparency. More details are described elsewhere [13]. The thickness of the bottom layer, the separating layer and the top layer are all 100 nm. The substrate ramp is quite broad and reaches outside of Fig. 8. The slope of the substrate ramp is 8°. The YBCO film is oriented with the c-axis perpendicular to the substrate surface both outside and in the ramp area. As the c-axis of the film is perpendicular to the inclined surface, there is an 8° misalignment between the film to the left and to the right in the figure. This orientation difference is accommodated by a grain boundary and a few microcracks. A reaction layer ($BaZrO_3$) between YBCO and YSZ substrate is observed along the whole interface. On the inclined surface there is an amorphous layer between YBCO and YSZ substrate. The top layer and the barrier layer are full of defects (planar defects) compared to the bottom YBCO layer and the separating layer. Because of this difference one can approximately locate the barrier layer. However, the exact position and the width of the barrier layer cannot be measured. An a-axis oriented YBCO grain can be observed in the junction area, starting in the lower part and continuing in the top YBCO film.

Fig. 9 shows a low-magnification image in plane view of the ramp-edge junction from the same sample as shown in Figs. 2 and 3. The figure presents a view through the multilayer film in the ramp area. It is difficult to locate the junction exactly, but the junction must be around where the contrast changes from dark to bright. The dark and bright areas correspond to the four-layer and two-layer part, respectively. Over this 1 μm projection of the ramp, the film shows no defect except some a orientation grains in the four-layer film. The defects in the top YBCO layer in the four-layer side does not influence the quality of the junction.

4. Discussion

Ramp-edge junctions on $SrTiO_3$, $NdGaO_3$, and YSZ substrates have been characterized by HREM investigations of cross-section specimens. The ramp-edge junctions are schematically represented in Fig. 1. The TEM results confirm the as-designed configuration of the junction except for the YSZ substrate. This indicates that the used fabrication process can result in a high-quality Josephson junction provided the right substrate is used.

In order to make sure that the bottom superconducting layer YBCO (or DyBCO) is removed by the JJ ion milling, usually a little more JJ ion milling is performed such that a step and sometimes a dimple is formed on the surface of the substrate as shown in Fig. 5. Such a change in the slope can influence the fabrication of a ramp-edge junction. If the substrate is perovskite-like, such as $SrTiO_3$, $NdGaO_3$ $LaAlO_3$, and $LaGaO_3$, good epitaxy can be obtain through the multi-component film on the ramp in the substrate. Fig. 10 shows an YBCO thin film grows on a step of $LaAlO_3$ substrate with an angle of about 30°. As shown previously [8], or YBCO thin film can grow epitaxially on a step (step angle less than 40°) with (001) plane of YBCO parallel to that of substrate provided it is a perovskite-like substrate. When the step angle is around 45°, a mix of a and c oriented film can grow on the step as shown in Fig. 11. In the case of YSZ substrate, the YBCO film grows on the YSZ substrate with the c-axis perpendicular to the substrate surface because of the intermediate layer of $BaZrO_3$ (as shown in Fig. 8 of Ref. [14]). For an MgO substrate with a step, YBCO behaves as on YSZ substrate [15]. Therefore, grain boundaries and microcracks easily occur at the tip of the ramp to accommodate the slope-angle change between the ramp and the bottom of YSZ and MgO substrate. These defects have their own electrical characteristics, which will deteriorate the performance of the device. In the case of the perovskite-type substrates $SrTiO_3$, $LaAlO_3$, and $NdGaO_3$, the epitaxial growth of YBCO on the ramp enables the barrier layer to have the same orientation as the neighboring YBCO layers such that no discontinuities occur. Therefore, only these substrates with perovskite-type structure is suitable to fabricate ramp-type junctions.

Perfect c oriented film growth is the basic requirement for a successful fabrication of a ramp-edge junction. The dominant reason for preventing the occurrence of a oriented grains is the surface roughening, which will be the result of the large growth

rates along the a–b plane compared to that along c-axis. Normally a oriented instead of c oriented growth will occur on an c oriented grain resulting in a continuation of the a orientation up to the film surface. In particularly an a oriented grain in the bottom layer will have a detrimental effect on the performance of the device because of several reasons:

(1) An a oriented grain in four-layer area may form a leakage between the top and the bottom superconducting layers through the a oriented grain. A thick separating PrBCO and SrTiO$_3$ layer can prevent this leakage. In the investigated specimens the thickness of the separating layer was adequate to prevent the leakage.

(2) An a oriented grain in the junction area will certainly lead to a local variation in the thickness of the barrier layer thus deteriorating the properties of the junction. Fig. 8 shows an example.

(3) During JJ ion milling an a oriented outgrowth can result in more or less steep steps on the substrate. Therefore, the smoothness of the two-layer part is determined by the original smoothness of the bottom YBCO layer even if this was JJ ion milled away. These steps could be steep enough to introduce grain boundaries in the two-layer film.

On the ramp surface created by JJ ion milling the barrier PrBCO layer and the top YBCO have to be grown epitaxially without any defects (for instance grain boundaries, a oriented grains, and microcracks) which can affect the characteristic of junctions. In the case of PrBCO as separating layer, full epitaxially growth of the barrier layer PrBCO can be obtained on the ramp surface which can be expected because there is no change in structure. Also in the case of SrTiO$_3$ as separating layer the barrier layer PrBCO can grow epitaxially on the ramp surface even through the structures of PrBCO and SrTiO$_3$ are different. In this respect it will be interesting to check the influence of ZrO$_2$ or MgO as separating layer. The PrBCO barrier layer will have a preference to grow with the c-axis perpendicular to the inclined ZrO$_2$ and MgO surface (present at the ramp) which might result in a degradation of the barrier layer in the Josephson junction area [16].

The most important part in the ramp-edge junction is the barrier layer. The other junctions from the same multi-junction sample show the same junction

geometry. From Figs. 3 and 5 one can see that the barrier layer is more or less homogeneous. This indicates that it is feasible to control the thickness of the barrier layer. Also no grain boundaries within the barrier layer could be seen. The barrier layer can epitaxially grow on the JJ ion milling edge surface.

On a multi-junction sample, there are always two types of ramps of which one is facing towards and the other is facing away from the ion-milling gun. For these two types, different substrate ramps and dimples will be formed. The removed substrate on the side which is facing towards JJ ion gun is lower than that on the opposite side. A dimple is created when the ramp is facing away from the ion gun, while there is no dimple when the ramp is facing towards the ion gun. The formation of this dimple can be understood if one considers that when the incident angle of ions is at a grazing angle to the surface of the ramp, a part of the ions will be reflected resulting in a higher flux of ions at the bottom of the ramp. This higher flux will create a dimple in the substrate at the bottom of ramp. The slopes in the dimples we have investigated were not larger than about 30°; in all cases the YBCO film was still epitaxially grown in the dimple.

The barrier layers of the ramps facing the ion gun have in general less sharp interfaces. This is probably due to the more severe and deeper damage created by the ion milling since the incidence angle is about 70° compared to less than 10° on the ramp facing away from the ion gun. It is not clear whether the less sharp interface will have a bad influence on the performance of the Josephson junction.

5. Conclusion

A ramp-edge YBCO/PrBCO/YBCO Josephson junction can be imaged by HREM. The barrier layer is observed to have a homogeneous thickness. A step on the substrate close to the base of junction is always observed. In the case of a YSZ substrate, the slopes of the step on the substrate were found to lead to small-angle grain boundaries and completely differently oriented YBCO grains, thus resulting in a poor ramp-edge junction. In the case of a SrTiO$_3$ or NdGaO$_3$ substrate, all components of the device are fully epitaxial, thus resulting in a good ramp-edge

junctions. The choice of substrate is very important. TEM results confirm that the ramp-edge Josephson junction appear to be as was intended.

Acknowledgements

References

[1] A.L. Braginski, Physica C 158–189 (1991) 391.
[2] D. Dimos, P. Chaudhari, J. Mannhart and F.K. LeGoues, Phys. Rev. Lett. 61 (1988) 219.
[3] K. Char, M.S. Colclough, S.M. Garrison, N. Newman and G. Zaharchuk, Appl. Phys. Lett. 59 (1991) 733.
[4] K. Herrmann, Y. Zhang, H.-M. Muck, J. Schubert, W. Zander and A.I. Braginski, Supercond. Sci. Technol. 4 (1991) 583.
[5] O.I. Lebedev, A.L. Vasiliev, N.A. Kiselev, L.A. Mazo, S.V. Gaponov, D.G. Paveliev and M.D. Strikovsky, Physica C 198 (1992) 583.
[6] C.L. Jia, B. Kabius, K. Urban, K. Herrmann, G.J. Cui, J. Schubert, W. Zander, A.I. Braginski and C. Heiden, Physica C 175 (1991) 545.
[7] C.L. Jia, B. Kabius, K. Urban, K. Herrmann, J. Schubert, W. Zander and A.I. Braginski, Physica C 196 (1992) 211.
[8] J.G. Wen, C. Traeholt and H.W. Zandbergen, Physica C 205 (1993) 354.
[9] J. Gao, Yu.M. Boguslavskij, B.B.G. Klopman, D. Terpstra, R. Wijbrans, G.J. Gerritsma and H. Rogalla, J. Appl. Phys. 72 (1992) 575.
[10] J. Gao, W.A.M. Aarnink, G.J. Gerritsma and H. Rogalla, Physica C 171 (1990) 126.
[11] J. Gao, W.A.M. Aarnink, G.J. Gerritsma, D. Veldhuis and H. Rogalla, IEEE Trans. Magn. (1992) 3062.
[12] C. Traeholt, J.G. Wen, V. Svetchnikov, A. Delsin and H.W. Zandbergen, Physica C 206 (1993) 318.
[13] J.G. Wen, in: From the macroscopic to the atomic scale: Charactersation of high-T_c superconductors by electron microscopy, Chapter 4, eds. N.D. Browning and S.J. Pennycook, to be published.
[14] J.G. Wen, C. Traeholt, H.W. Zandbergen, K. Joosse, E.M.C.M. Reuvekamp and H. Rogalla, Physica C 218 (1993) 29.
[15] T. Matsuzuka, K. Yamaguchi, S. Yoshikawa, K. Hayashi, M. Konishi and Y. Enomoto, Physica C 218 (1993) 229.
[16] J.B. Barner, B.D. Hunt, M.C. Foote, W.T. Pike and R.P. Vasquez, Physica C 207 (1993) 381.